

Article

Synthesis and Compressibility of Novel Nickel Carbide at Pressures of Earth's Outer Core

Timofey Fedotenko ^{1,*}, Saiana Khandarkhaeva ¹, Leonid Dubrovinsky ² , Konstantin Glazyrin ³ , Pavel Sedmak ⁴ and Natalia Dubrovinskaia ^{1,5} 

- ¹ Material Physics and Technology at Extreme Conditions, Laboratory of Crystallography, University of Bayreuth, D-95440 Bayreuth, Germany; saiana.khandarkhaeva@uni-bayreuth.de (S.K.); natalia.dubrovinskaia@uni-bayreuth.de (N.D.)
- ² Bayerisches Geoinstitut, University of Bayreuth, D-95440 Bayreuth, Germany; leonid.dubrovinsky@uni-bayreuth.de
- ³ Deutsches Elektronen Synchrotron, 22607 Hamburg, Germany; konstantin.glazyrin@desy.de
- ⁴ European Synchrotron Radiation Facility, F-38043 Grenoble, France; pavel.sedmak@anton-paar.com
- ⁵ Department of Physics, Chemistry and Biology (IFM), Linköping University, SE-581 83 Linköping, Sweden
- * Correspondence: timofeyfedotenko@gmail.com

Abstract: We report the high-pressure synthesis and the equation of state (EOS) of a novel nickel carbide (Ni₃C). It was synthesized in a diamond anvil cell at 184(5) GPa through a direct reaction of a nickel powder with carbon from the diamond anvils upon heating at 3500 (200) K. Ni₃C has the cementite-type structure (Pnma space group, $a = 4.519(2)$ Å, $b = 5.801(2)$ Å, $c = 4.009(3)$ Å), which was solved and refined based on in-situ synchrotron single-crystal X-ray diffraction. The pressure-volume data of Ni₃C was obtained on decompression at room temperature and fitted to the 3rd order Burch-Murnaghan equation of state with the following parameters: $V_0 = 147.7(8)$ Å³, $K_0 = 157(10)$ GPa, and $K_0' = 7.8(6)$. Our results contribute to the understanding of the phase composition and properties of Earth's outer core.

Keywords: nickel carbide; high pressures; X-ray diffraction; equation of state; Earth's outer core



Citation: Fedotenko, T.; Khandarkhaeva, S.; Dubrovinsky, L.; Glazyrin, K.; Sedmak, P.; Dubrovinskaia, N. Synthesis and Compressibility of Novel Nickel Carbide at Pressures of Earth's Outer Core. *Minerals* **2021**, *11*, 516. <https://doi.org/10.3390/min11050516>

Academic Editor: Fumagalli Patrizia

Received: 16 April 2021

Accepted: 10 May 2021

Published: 13 May 2021

Publisher's Note: MDPI stays neutral with regard to jurisdictional claims in published maps and institutional affiliations.



Copyright: © 2021 by the authors. Licensee MDPI, Basel, Switzerland. This article is an open access article distributed under the terms and conditions of the Creative Commons Attribution (CC BY) license (<https://creativecommons.org/licenses/by/4.0/>).

1. Introduction

Nickel is known as the second most abundant element in Earth's core after iron [1,2]. Cosmochemical models and studies of meteorites suggest that Earth's core apart from Fe contains also about 5 wt.% of Ni [3,4] and, in the inner core, up to 10 wt.% of light elements [5–7]. Which elements exactly and their amount is a subject of active discussions [3]. A large amount of carbon in iron meteorites [8], its high solubility in liquid Fe at high pressure [5,9], and high abundance in the solar system [5] suggest carbon to be one of the most important light elements in Earth's core. Recent estimations of the inner core composition indicate up to 2.0 wt.% of carbon [3]. All these facts resulted in numerous high-pressure studies of the Fe-C system in recent decades. The intermediate Fe-C compounds Fe₃C and Fe₇C₃ were suggested to be the most likely candidates to the carbon-bearing phases in Earth's core, as they were found at relevant pressures and temperatures [2,5,10–12]. Although at room temperature Fe₃C was shown to be stable up to 187 GPa, it decomposes into a mixture of solid Fe₇C₃ and hcp-Fe at above 145 GPa upon laser heating and transforms into Fe-C liquid and solid Fe₇C₃ at temperatures of above 3400 K [13]. Moreover, the high Poisson's ratio of Fe₇C₃ at high pressures [2] indicates that the presence of carbon may significantly affect the elastic properties of iron. This corroborates the Preliminary Reference Earth Model (PREM) [14], which suggests the material of Earth's inner core also has a high Poisson's ratio.

Contrary to the binary iron-carbon system, the Fe-Ni-C, and Ni-C systems at high PT conditions are still poorly understood. Nickel can strongly modify the physical properties of pure Fe at elevated pressures and temperatures. Recent studies have shown that Ni

alloying on Fe does not affect the melting temperature of Fe up to 100 GPa; however, it modifies its phase boundary by shifting the hcp/fcc/liquid triple point to the higher pressure-temperature region [6]. For example, for Fe-20 wt.% Ni alloy the triple point was found to be at 170(20) GPa and 4000(400) K [6] as compared to 100(10) GPa and 3500(200) K for pure Fe [15]. Pressure-induced Invar effect in Fe-Ni alloys was reported by Dubrovinsky et al. [16]. The thermal expansion of the alloys $\text{Fe}_{0.55}\text{Ni}_{0.45}$ and $\text{Fe}_{0.20}\text{Ni}_{0.80}$ was found to be extremely low in the temperature interval of 291 K to 500 K at pressures of 7.7 and 12.6 GPa, correspondingly [16]. It was also proven that alloys of Fe with Ni have significantly higher strength in comparison with pure Fe [17]. The mineral cohenite, $(\text{Fe}, \text{Ni})_3\text{C}$, which is isostructural to Fe_3C , was found in iron meteorites [18] and predicted to be stable at high pressures [19]. However, a pure-Ni cementite-type phase (Ni_3C) has never been reported before.

Here, we report the synthesis and EOS of a novel high-pressure phase of nickel carbide (Ni_3C) in a laser-heated diamond anvil cell (LHDAC) at 184(5) GPa and 3500(200) K which was solved and refined using in-situ synchrotron single-crystal X-ray diffraction.

2. Materials and Methods

In our experiments, we used the BX90-type large X-ray aperture Diamond Anvil Cell (DAC) equipped with Boehler–Almax type diamonds with 80 μm culet diameter. To form the sample chamber, a rhenium gasket was preindented to ~ 20 μm thickness and a hole of 40 μm in diameter was drilled at the center of the indentation. A nickel powder was clamped between two thin layers of LiF inside the DAC's sample chamber. LiF played a role of a pressure transmitting and thermal insulating medium in order to decrease temperature gradients in the sample during laser heating [20]. The pressure was determined using the equations of states (EOSes) of Ni [21] and monitored additionally using Raman signal from the diamond anvils [22].

The laser-heating (LH) of the samples was performed using in house laser heating setup [23]. The double-sided LH system is equipped with two YAG lasers (1064 nm central wavelength) and the IsoPlane SCT 320 spectrometer with a 1024×2560 PI-MAX 4 camera for the collection of thermal emission spectra from the heated spot. Temperatures were determined by fitting of thermal emission spectra of the sample to the grey body approximation of Planck's radiation function in a given wavelength range (570–830 nm).

High-pressure single-crystal and powder X-ray diffraction (SCXRD) experiments were carried out at the extreme conditions beamline P02.2 (DESY, Hamburg, Germany) [24] and material science beamline ID11 (ESRF, Grenoble, France). The following beamline setups were used: At P02.2, $\lambda = 0.29$ Å, the beam size $\sim 2 \times 2$ μm^2 , a Perkin Elmer XRD 1621 detector; at ID11, $\lambda = 0.30996$ Å, the beam size $\sim 0.5 \times 0.5$ μm^2 , a Frelon4M detector. Single-crystal XRD data were collected during rotation of the DAC around the vertical ω -axis in a range $\pm 35^\circ$. The diffraction images were collected with an exposure time of 5 s per frame with an angular step $\Delta\omega = 0.5^\circ$.

To analyze the SCXRD data we used the CrysAlisPro software [25]. The analysis procedure includes the peak search, finding reflections belonging to a unique single-crystal domain, indexing, and data integration. The crystal structures were solved using ShelXT [26] structure solution program and refined with the JANA 2006 software [27].

Powder diffraction measurements were performed either without or upon continuous sample rotation about the ω axis of a diffractometer in the range of $\pm 20^\circ$. The images were integrated into powder patterns with Dioptas software [28] and analyzed with Le Bail fitting technique using TOPAS 4.2. The parameters of the equation of state were obtained by fitting the pressure–volume data using EoSFit7-GUI software [29].

3. Results and Discussion

Sample of Ni powder was pressurized in LiF pressure-transmitting medium up to 184(5) GPa and laser-heated up to 3500 (200) K by scanning of the Ni sample with a laser

\AA , $c = 4.009(4) \text{\AA}$ at 184(5) GPa) and the Ni_3C chemical composition (Table 1, Supplementary Material, Crystallographic Information File: $\text{Ni}_3\text{C}_{184\text{GPa.cif}}$).

Table 1. Crystallographic data for the Ni_3C at 184(5) GPa and 293 K.

Chemical Formula	Ni_3C
Crystal system	Orthorhombic
Space group	Pnma
Pressure (GPa)	184(5)
Temperature (K)	293
a (\AA)	4.520(3)
b (\AA)	5.8014(17)
c (\AA)	4.009(4)
V (\AA^3)	105.12(13)
Z	4
Density($\text{g}\cdot\text{cm}^{-3}$)	11.884
Radiation type	synchrotron, $\lambda = 0.2895 \text{\AA}$
Diffractometer	P02.2 @DESY
No. of measured, Independent and observed [$I > 3\sigma(I)$] reflections	366, 182, 83
Rint	7.3%
Refinement method	Full matrix least-squares on F
R [$F > 3\sigma(F)$], wR(F), S	6.43, 8.42, 1.43
No. of parameters	19
$\Delta\rho_{\text{max}}$, $\Delta\rho_{\text{min}}$ ($\text{e}\cdot\text{\AA}^{-3}$)	3.09, -3.51

The structure can be described as built of distorted trigonal prisms formed by six nickel atoms coordinating a C atom (Figure 3). The Ni-C distances in the prism vary from 1.760(19) to 1.830(16) \AA at 184(5) GPa. The trigonal prisms, interconnected through sharing edges and corners, form layers parallel to the ac plane stacking along the b direction. The previously observed trigonal Ni_3C (R-3c space group), which is a product of the thermal decomposition of Ni succinate [30] is built of CNi_6 octahedra with an average Ni-C distance of 1.86 \AA . Thus, the average Ni-C distance depends on the coordination of C atoms. Our data suggest that at ambient pressure the average Ni-C distance in CNi_6 trigonal prisms should be significantly larger compared to that in CNi_6 octahedra.

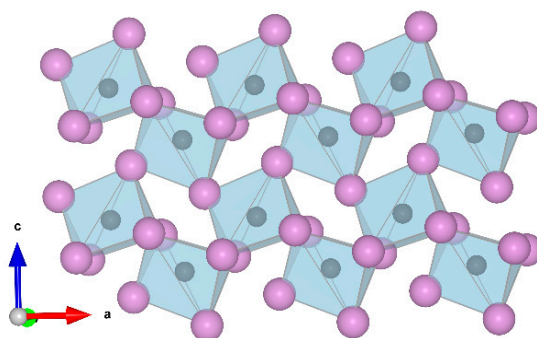


Figure 3. Crystal structure of the cementite type Ni_3C at 184(5) GPa and room temperature. Purple and black spheres designate nickel and carbon atoms, correspondingly.

The Ni_3C sample was studied on a stepwise decompression. SCXRD data were collected at seven pressure points down to 84(2) GPa. Below 84(2) GPa no diffraction pattern from Ni_3C was observed; however, the reason remained unclear. That means the question as to if the quality of the sample deteriorated or the phase decomposed or amorphized stays open. The pressure-volume data (Table 2) of Ni_3C was fitted to the 3rd order Birch-Murnaghan (BM3) EOS and gave the following parameters: $V_0 = 147.7(8) \text{\AA}^3$; $K_0 = 157(10) \text{GPa}$, $K' = 7.8(6)$ (Figure 4).

Table 2. The pressure dependence of the unit cell parameter of Ni₃C. Values in parentheses correspond to experimental uncertainties.

Pressure, GPa	Volume, Å ³
84(2)	117.1(6)
101(2)	114.7(3)
123(3)	111.7(4)
142(3)	108.9(4)
160(4)	107.4(4)
170(4)	106.3(3)
184(5)	105.1(2)

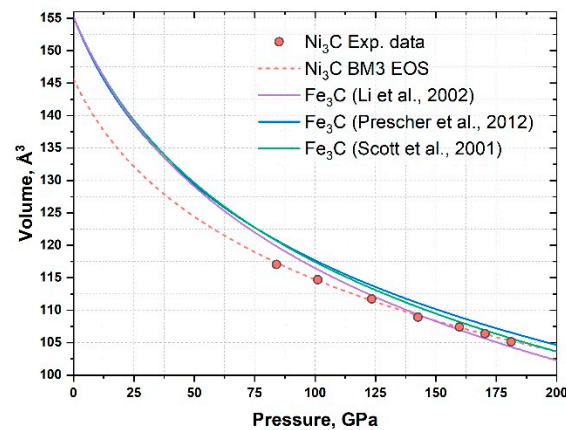


Figure 4. The pressure-volume dependence of Ni₃C. Red dots represent experimental data, the dashed red curve is the BM3 EOS fit ($V_0 = 147.7(8) \text{ \AA}^3$; $K_0 = 157(10) \text{ GPa}$, $K' = 7.8(6)$). Solid purple, blue and green lines correspond to the EOSes of Fe₃C from studies of Li et al. ($K_0 = 174(6) \text{ GPa}$, $K' = 4.8(8)$) [31], Prescher et al. ($K_0 = 161(2) \text{ GPa}$, $K' = 5.9(2)$) [32] and Scott et al. ($K_0 = 165(4) \text{ GPa}$, $K' = 5.99(9)$) [33].

Figure 5 demonstrates experimental data on Ni₃C axial compression. The structure is most compressible along the b axis, the direction of stacking of the layers of interconnected CNi₆ trigonal prisms. Compared to the predicted compressional behavior of Fe₃C in the same pressure region [34], Ni₃C is highly anisotropic.

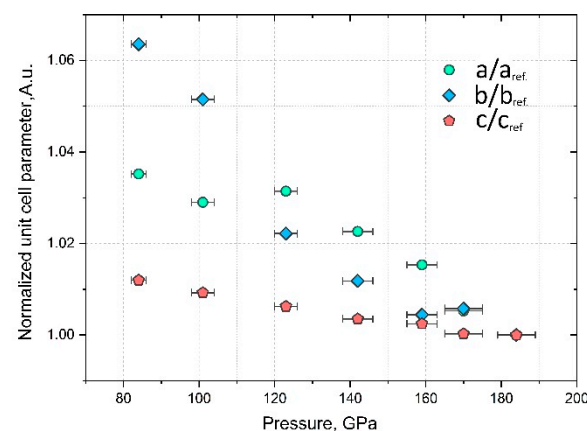


Figure 5. The pressure dependence of the normalized unit cell parameters of Ni₃C at 300 K.

Based on obtained data, we calculated the bulk sound velocity for Ni₃C as a function of pressure at 293 K and compared it with those known for Fe, Ni, and possible carbon-

bearing components of Earth's core (Fe_3C and Fe_7C_3). Figure 6 shows that within the errors Ni_3C exhibits similar bulk velocities as Fe_3C and Fe_7C_3 at pressures up to 400 GPa.

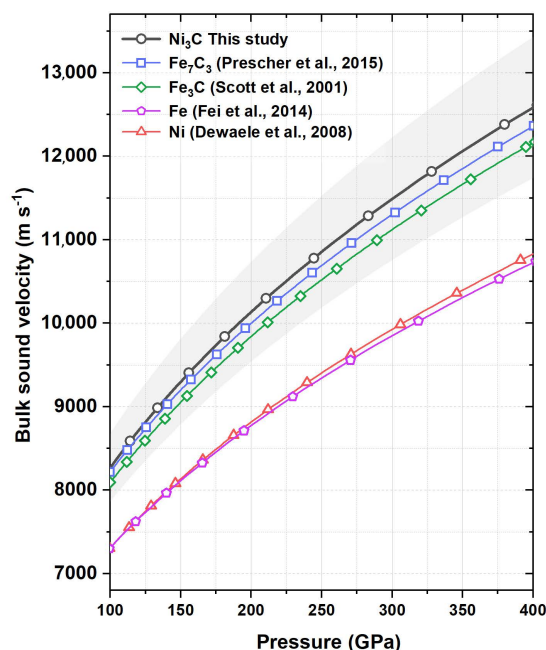


Figure 6. Calculated bulk sound velocity as a function of pressure for Ni_3C (this study, black solid line with circles); Fe_3C (green line with diamonds [33]) and Fe_7C_3 (blue line with squares [2]); Ni (red line with triangles [21]); Fe (purple line with pentagons [35]) at 293 K.

Thereby, the presence of Ni in the alloy likely should not affect the elastic properties of the Fe-Ni-C system at high pressure but potentially can change the carbon distribution. Due to the stability of Ni_3C at conditions of Earth's outer core, it may be considered as one of the likely candidates to carbon-bearing phases in the core along with Fe_7C_3 .

4. Conclusions

In the presented work, we have synthesized a nickel carbide yet unknown at ambient conditions. It was shown that Ni reacts with carbon at high-pressure and high-temperature conditions that result in the formation of an orthorhombic Ni_3C compound (space group Pnma, $a = 4.520(3)$ Å, $b = 5.8014(17)$ Å, $c = 4.009(4)$ Å at 84(5) GPa) with the cementite-type structure revealed using synchrotron single-crystal X-ray diffraction. The Ni_3C was studied on decompression down to 84(2) GPa. We have shown that in the pressure range 84(2)–185(5) GPa, Ni_3C is less compressible than cementite (Fe_3C); the calculated bulk sound velocities are similar to those known for Fe_3C and Fe_7C_3 at pressures up to 400 GPa and 297 K. Ni_3C remains stable at pressure-temperature conditions relevant to Earth's core and thus can be considered as one of the likely candidates to carbon-bearing phases in the core along with Fe_7C_3 .

Supplementary Materials: The following are available online at <https://www.mdpi.com/article/10.3390/min11050516/s1>, Crystallographic information file of Ni_3C at 184(5) GPa.

Author Contributions: Conceptualization, T.F., L.D. and N.D.; methodology, T.F. and S.K.; validation, T.F. and S.K.; formal analysis, T.F.; investigation, T.F., S.K., K.G., P.S.; data curation, T.F.; writing—original draft preparation, T.F.; writing—review and editing, N.D. and L.D.; visualization, T.F.; supervision, N.D. and L.D.; project administration, T.F. and L.D.; funding acquisition, N.D. and L.D. All authors have read and agreed to the published version of the manuscript.

Funding: N.D. and L.D. thank the Federal Ministry of Education and Research, Germany (BMBF, grant No. 05K19WC1) and the Deutsche Forschungsgemeinschaft (DFG projects DU 954-11/1, DU

393-9/2, and DU 393-13/1) for financial support. N.D. thanks the Swedish Government Strategic Research Area in Materials Science on Functional Materials at Linköping University (Faculty Grant SFO-Mat-LiU No. 2009 00971).

Institutional Review Board Statement: Not applicable.

Informed Consent Statement: Not applicable.

Data Availability Statement: The data that support the findings of this study are available from the corresponding author upon reasonable request.

Acknowledgments: We acknowledge DESY (Hamburg, Germany), a member of the Helmholtz Association HGF, for the provision of experimental facilities, photon beamline P02.2 (Petra III).

Conflicts of Interest: The authors declare no conflict of interest.

References

- Birch, F. Elasticity and constitution of the Earth's interior. *J. Geophys. Res.* **1952**, *57*, 227–286. [[CrossRef](#)]
- Prescher, C.; Dubrovinsky, L.; Bykova, E.; Kuppenko, I.; Glazyrin, K.; Kantor, A.; McCammon, C.; Mookherjee, M.; Nakajima, Y.; Miyajima, N.; et al. High Poisson's ratio of Earth's inner core explained by carbon alloying. *Nat. Geosci.* **2015**, *8*, 220–223. [[CrossRef](#)]
- Litasov, K.D.; Shatskiy, A.F. Composition of the Earth's core: A review. *Russ. Geol. Geophys.* **2016**, *57*, 22–46. [[CrossRef](#)]
- McDonough, W.F. Compositional Model for the Earth's Core. In *Treatise on Geochemistry*; Elsevier: Amsterdam, The Netherlands, 2003; pp. 547–568.
- Wood, B.J. Carbon in the core. *Earth Planet. Sci. Lett.* **1993**, *117*, 593–607. [[CrossRef](#)]
- Torchio, R.; Boccatto, S.; Miozzi, F.; Rosa, A.D.; Ishimatsu, N.; Kantor, I.; Sévelin-Radiguet, N.; Briggs, R.; Meneghini, C.; Irifune, T.; et al. Melting Curve and Phase Relations of Fe-Ni Alloys: Implications for the Earth's Core Composition. *Geophys. Res. Lett.* **2020**, *47*, e2020GL088169. [[CrossRef](#)]
- Poirier, J.-P. Light elements in the Earth's outer core: A critical review. *Phys. Earth Planet. Inter.* **1994**, *85*, 319–337. [[CrossRef](#)]
- Bashir, N.; Beckett, J.R.; Hutcheon, I.D.; Stolper, E.M. Carbon in the Metal of Iron Meteorites. In Proceedings of the Lunar and Planetary Science Conference, Houston, TX, USA, 18–22 March 1996; Volume 27, p. 63.
- Hirayama, Y.; Fujii, T.; Kurita, K. The melting relation of the system, iron and carbon at high pressure and its bearing on the early stage of the Earth. *Geophys. Res. Lett.* **1993**, *20*, 2095–2098. [[CrossRef](#)]
- Lord, O.T.; Walter, M.J.; Dasgupta, R.; Walker, D.; Clark, S.M. Melting in the Fe-C system to 70 GPa. *Earth Planet. Sci. Lett.* **2009**, *284*, 157–167. [[CrossRef](#)]
- Nakajima, Y.; Takahashi, E.; Suzuki, T.; Funakoshi, K. "Carbon in the core" revisited. *Phys. Earth Planet. Inter.* **2009**, *174*, 202–211. [[CrossRef](#)]
- Chen, B.; Li, Z.; Zhang, D.; Liu, J.; Hu, M.Y.; Zhao, J.; Bi, W.; Alp, E.E.; Xiao, Y.; Chow, P.; et al. Hidden carbon in Earth's inner core revealed by shear softening in dense Fe₇C₃. *Proc. Natl. Acad. Sci. USA* **2014**, *111*, 17755–17758. [[CrossRef](#)]
- Liu, J.; Lin, J.-F.; Prakapenka, V.B.; Prescher, C.; Yoshino, T. Phase relations of Fe₃C and Fe₇C₃ up to 185 GPa and 5200 K: Implication for the stability of iron carbide in the Earth's core. *Geophys. Res. Lett.* **2016**, *43*, 12415–12422. [[CrossRef](#)]
- Dziewonski, A.M.; Anderson, D.L. Preliminary reference Earth model. *Phys. Earth Planet. Inter.* **1981**, *25*, 297–356. [[CrossRef](#)]
- Morard, G.; Boccatto, S.; Rosa, A.D.; Anzellini, S.; Miozzi, F.; Henry, L.; Garbarino, G.; Mezouar, M.; Harmand, M.; Guyot, F.; et al. Solving Controversies on the Iron Phase Diagram Under High Pressure. *Geophys. Res. Lett.* **2018**, *45*, 11–074. [[CrossRef](#)]
- Dubrovinsky, L.; Dubrovinskaia, N.; Abrikosov, I.A.; Vennström, M.; Westman, F.; Carlson, S.; van Schilfgaarde, M.; Johansson, B. Pressure-Induced Invar Effect in Fe-Ni Alloys. *Phys. Rev. Lett.* **2001**, *86*, 4851–4854. [[CrossRef](#)] [[PubMed](#)]
- Reagan, M.M.; Gleason, A.E.; Liu, J.; Krawczynski, M.J.; Van Orman, J.A.; Mao, W.L. The effect of nickel on the strength of iron nickel alloys: Implications for the Earth's inner core. *Phys. Earth Planet. Inter.* **2018**, *283*, 43–47. [[CrossRef](#)]
- Brett, R. Cohenite in Meteorites: A Proposed Origin. *Science* **1966**, *153*, 60–62. [[CrossRef](#)]
- Ringwood, A.E. Cohenite as a pressure indicator in iron meteorites. *Geochim. Cosmochim. Acta* **1960**, *20*, 155–158. [[CrossRef](#)]
- Dong, H.; Dorfman, S.M.; Holl, C.M.; Meng, Y.; Prakapenka, V.B.; He, D.; Duffy, T.S. Compression of lithium fluoride to 92 GPa. *High Press. Res.* **2014**, *34*, 39–48. [[CrossRef](#)]
- Dewaele, A.; Torrent, M.; Loubeyre, P.; Mezouar, M. Compression curves of transition metals in the Mbar range: Experiments and projector augmented-wave calculations. *Phys. Rev. B* **2008**, *78*, 104102. [[CrossRef](#)]
- Akahama, Y.; Kawamura, H. Pressure calibration of diamond anvil Raman gauge to 310GPa. *J. Appl. Phys.* **2006**, *100*, 043516. [[CrossRef](#)]
- Fedotenko, T.; Dubrovinsky, L.; Aprilis, G.; Koemets, E.; Snigirev, A.; Snigireva, I.; Barannikov, A.; Ershov, P.; Cova, F.; Hanfland, M.; et al. Laser heating setup for diamond anvil cells for in situ synchrotron and in house high and ultra-high pressure studies. *Rev. Sci. Instrum.* **2019**, *90*, 104501. [[CrossRef](#)]

24. Liermann, H.-P.; Konôpková, Z.; Morgenroth, W.; Glazyrin, K.; Bednarčík, J.; McBride, E.E.; Petitgirard, S.; Delitz, J.T.; Wendt, M.; Bican, Y.; et al. The Extreme Conditions Beamline P02.2 and the Extreme Conditions Science Infrastructure at PETRA III. *J. Synchrotron Radiat.* **2015**, *22*, 908–924. [[CrossRef](#)]
25. CrysAlis Pro (v. 171.39.46). Available online: <https://www.rigaku.com/products/smc/crysalis> (accessed on 3 January 2020).
26. Sheldrick, G.M. SHELXT—Integrated space-group and crystal-structure determination. *Acta Crystallogr. Sect. A Found. Adv.* **2015**, *71*, 3–8. [[CrossRef](#)] [[PubMed](#)]
27. Petříček, V.; Dušek, M.; Plášil, J. Crystallographic computing system Jana2006: Solution and refinement of twinned structures. *Zeitschrift für Krist. Cryst. Mater.* **2016**, *231*, 583–599. [[CrossRef](#)]
28. Prescher, C.; Prakapenka, V.B. DIOPTAS: A program for reduction of two-dimensional X-ray diffraction data and data exploration. *High Press. Res.* **2015**, *35*, 223–230. [[CrossRef](#)]
29. Gonzalez-Platas, J.; Alvaro, M.; Nestola, F.; Angel, R. EosFit7-GUI: A new graphical user interface for equation of state calculations, analyses and teaching. *J. Appl. Crystallogr.* **2016**, *49*, 1377–1382. [[CrossRef](#)]
30. Huba, Z.J.; Carpenter, E.E. Monitoring the formation of carbide crystal phases during the thermal decomposition of 3d transition metal dicarboxylate complexes. *Dalt. Trans.* **2014**, *43*, 12236–12242. [[CrossRef](#)]
31. Li, J.; Mao, H.K.; Fei, Y.; Gregoryanz, E.; Eremets, M.; Zha, C.S. Compression of Fe₃C to 30 GPa at room temperature. *Phys. Chem. Miner.* **2002**, *29*, 166–169. [[CrossRef](#)]
32. Prescher, C.; Dubrovinsky, L.; McCammon, C.; Glazyrin, K.; Nakajima, Y.; Kantor, A.; Merlini, M.; Hanfland, M. Structurally hidden magnetic transitions in Fe₃C at high pressures. *Phys. Rev. B* **2012**, *85*, 140402. [[CrossRef](#)]
33. Scott, H.P.; Williams, Q.; Knittle, E. Stability and equation of state of Fe₃C to 73 GPa: Implications for carbon in the Earth’s core. *Geophys. Res. Lett.* **2001**, *28*, 1875–1878. [[CrossRef](#)]
34. Mookerjee, M. Elasticity and anisotropy of Fe₃C at high pressures. *Am. Miner.* **2011**, *96*, 1530–1536. [[CrossRef](#)]
35. Fei, Y.; Murphy, C.; Shibasaki, Y.; Shahar, A.; Huang, H. Thermal equation of state of hcp-iron: Constraint on the density deficit of Earth’s solid inner core. *Geophys. Res. Lett.* **2016**, *43*, 6837–6843. [[CrossRef](#)]